

A&A manuscript no.
(will be inserted by hand later)

Your thesaurus codes are:
12.03.1, 12.04.2, 10.08.1, 09.12.1

Galactic H α emission and the Cosmic Microwave Background

M. Marcelin¹, P. Amram¹, J.G. Bartlett², D. Valls-Gabaud², and A. Blanchard²

¹ IGRAP, Observatoire de Marseille, 2 Place Le Verrier, 13248 Marseille Cedex 04, France

² Observatoire de Strasbourg, 11 rue de l'Université, 67000 Strasbourg, France

Received 15 May 1998 / Accepted 24 June 1998

Abstract. We present observations of Galactic H α emission along two declination bands where the South Pole cosmic microwave background experiment reports temperature fluctuations. The high spectral resolution of our Fabry–Perot system allows us to separate the Galactic signal from the much larger local sources of H α emission, such as the Earth's geocorona. For the two bands (at $\delta = -62^\circ$ and -63°), we find a total mean emission of ~ 1 R with variations of ~ 0.3 R. The variations are within the estimated uncertainty of our total intensity determinations. For an ionized gas at $T \sim 10^4$ K, this corresponds to a maximum free–free brightness temperature of less than $10 \mu\text{K}$ at 30 GHz (K–band). Thus, unless there is a hot gas component with $T \sim 10^6$ K, our results imply that there is essentially no free–free contamination of the SP91 (Schuster et al. 1993) and SP94 (Gunderson et al. 1995) data sets.

Key words: Cosmology: –cosmic microwave background, –diffuse radiation, Galaxy: –halo, ISM: lines and bands

1. Introduction

Cosmology has entered the era of precision cosmic microwave background (CMB) measurements. Since the original detection of temperature perturbations on large angular scales by the COBE satellite (Smoot et al. 1992), there has been a myriad of new detections, resulting in a data set spanning roughly two orders of magnitude in angular scale (Lineweaver et al. 1997; White et al. 1994). The extraction of cosmological information requires careful control and understanding of all possible sources of signal contamination. The current quest for high precision determination of cosmological parameters

Send offprint requests to: M. Marcelin

(Jungman et al. 1996; Knox 1995) demands a correspondingly greater understanding of all foregrounds. In particular, the Galaxy, via synchrotron, dust and free-free emission (Bremsstrahlung), represents a source of foreground brightness fluctuations which all experiments must reckon with. These three contaminating emissions define a “valley” in the brightness–frequency plane centered around 90 GHz, representing the point of smallest Galactic contamination (Kogut et al. 1996a). Although, clearly, CMB efforts are concentrated in this “valley”, Galactic signals must nonetheless be carefully removed to extract the purely cosmological fluctuations and to achieve the desired precision on cosmological parameters.

The removal of these foregrounds is usually done in one of two ways. With sufficient frequency coverage and a high signal-to-noise ratio, a spectral analysis of the CMB data alone can in principle distinguish the Galactic foregrounds from the CMB signal. The other approach is to use sky maps made at other frequencies as templates and to extrapolate a given foreground emission into the CMB bands according to its spectral dependence. Even when the quality of the CMB data permits the former technique, the second approach provides an important, *external* check on the removal procedure. For synchrotron emission, one usually uses the 408 MHz Haslam map (Haslam et al. 1981) and the 1420 MHz survey (Reich & Reich 1986) as a template (uncertain spatial variations of the synchrotron frequency index renders the procedure slightly less straightforward than one would hope). The IRAS all sky survey serves as a useful template for dust emission on angular scales under $\sim 1^\circ$, and it is usually augmented with DIRBE maps on larger angular scales (as with synchrotron emission, uncertainty in the exact slope of the dust emission law introduces an unfortunate complication).

In this paper, we address the question of Galactic free-free emission in relation to CMB anisotropy measurements (two recent reviews are given by Smoot 1998 and Bartlett & Amram 1998). Among the three Galactic sources of troublesome microwave emission, free-free emission is the most difficult to control. This is because the only frequency range in which it dominates over dust and synchrotron emission is in the CMB valley; in other words, one cannot extrapolate maps made at much lower or higher frequencies into the CMB valley to remove free-free contamination. What is needed is a tracer of the warm ionized interstellar medium (WIM) responsible for free-free emission. Given that at high Galactic latitudes there is minimal extinction from dust, one expects Hydrogen H α line emission in the excited gas to be a good possibility for such a tracer.

The line emission is measured in Rayleighs ($1\text{R} = 10^6/4\pi \text{ photons cm}^{-2} \text{ s}^{-1} \text{ ster}^{-1} = 2.41 \times 10^{-7} \text{ erg cm}^{-2} \text{ s}^{-1} \text{ ster}^{-1}$ at $\lambda(H\alpha) = 6563 \text{ \AA}$) and may be expressed in terms of the temperature and emission measure, EM , of the WIM for Case B recombination:

$$I(H\alpha) \approx (0.36 \text{ R}) \left(\frac{EM}{\text{cm}^{-6} \text{ pc}} \right) T_4^{-0.9}, \quad (1)$$

where $T_4 \equiv T/10^4$ K; this expression is valid for temperatures $T_4 \leq 2.6$ (e.g. Reynolds 1990), more accurate formulae are given by Valls-Gabaud (1998). Free-free emission depends on the same quantities (given here for pure Hydrogen and in the limit as $h\nu/kT \rightarrow 0$):

$$T_b \approx \frac{(5.43 \mu\text{K})}{\nu_{10}^2 T_4^{1/2}} \left(\frac{EM}{\text{cm}^{-6} \text{ pc}} \right) g_{\text{ff}} \quad , \quad (2)$$

where T_b is the brightness temperature, the observation frequency is $\nu = \nu_{10}10^{10}$ Hz, and g_{ff} is the thermally averaged gaunt factor, which to 20% for $T_4 \leq \text{few}$ is

$$g_{\text{ff}} \sim 4.69(1 + 0.176 \ln T_4 - 0.118 \ln \nu_{10}) \quad , \quad (3)$$

(e.g. Smoot 1998). Thus, the free-free brightness associated with a given H α intensity is approximately

$$T_b \approx (15 \mu\text{K}) g_{\text{ff}} T_4^{0.4} \nu_{10}^{-2} \left(\frac{I(\text{H}\alpha)}{\text{R}} \right) \quad . \quad (4)$$

Valls-Gabaud (1998) discusses more accurate expressions. There does not, as of yet, exist a complete survey of the sky in H α , and the distribution of the warm ionized medium (WIM) of our galaxy remains somewhat of a mystery. Local sources pose the most serious difficulties for efforts to measure the Galactic H α emission. The Earth's geocorona emits in H α with an intensity of ~ 10 R, depending on the season, the solar activity and the solar depression angle. This is an order of magnitude larger than the typical signal we expect at high Galactic latitude. In addition, there is an OH line from the atmosphere at $\lambda = 6569$ Å. Fortunately, the Earth's motion through the Galaxy displaces the Galactic signal relative to the local H α emission, and thus the cleanest way to extract a Galactic signal is by use of a high-resolution spectrometer. Reynolds has developed this approach with a double Fabry-Perot system (Reynolds 1990) to study the Galactic emission on degree angular scales with pointed observations and a small-area survey below the Galactic Plane (Reynolds 1992; Reynolds 1980). This has culminated in the construction of WHAM (Wisconsin H α Mapper), which is currently surveying the entire northern sky at 1 degree resolution (see <http://www.astro.wisc.edu/wham/>).

Other groups have recently surveyed areas in the north using narrow band filters (Gaustad et al. 1996; Simonetti et al. 1996). This technique has the advantage of much greater simplicity and lower cost; the inconveniences are that one must remove the stellar contribution by extrapolation of off-band filters and that the Geocoronal H α emission cannot be subtracted correctly. Nevertheless, if the geocoronal H α emission is stable and uniform across the field-of-view (survey area) during the observations, then useful *upper limits* on the *anisotropy* of the Galactic signal can be obtained. Both Gaustad et al. (1996) and Simonetti et al. (1996) have placed limits on the possible contamination of

CMB observations at the North Celestial Pole and concluded that the Saskatoon (Wollack et al. 1997; Netterfield et al. 1997) experiment is unaffected by free–free contamination.

The situation is actually rather more complicated. Leitch et al. (1997) have recently reported the detection of a foreground signal around the NCP in data taken from the Owens Valley Radio Observatory. The signal has a spectral index favoring free–free emission, and it is well correlated with IRAS maps of the area. Such a correlation between free–free emission and dust emission has also been remarked by the COBE team in the DMR data at high Galactic latitudes (Kogut et al. 1996a; 1996b). If the foreground seen around the NCP is indeed due to Bremsstrahlung, then the intensity is 60 times larger than the limits implied by the narrow band observations in H α ! As discussed by Leitch et al. (1997), this could be explained by a gas at $T \sim 10^6$ K, instead of $T \sim 10^4$ K. It is interesting to note that 10^6 K is the virial temperature of our Galactic halo. Although difficult to understand how, another possibility is that the narrow band observations are missing something. A further possibility is that this signal is due to the rotational emission of very small spinning dust grains (Draine & Lazarian 1998). In any case, present data are not sufficient to yield a complete understanding of the importance of free–free contamination for CMB observations (Smoot 1998; Bartlett & Amram 1998).

In this paper, we present some of our H α observations at high galactic latitude in the Southern Hemisphere. The telescope and detector system were optimized for a survey of the Galactic Plane in H α at a resolution of 9 arcsecs (Le Coarer et al. 1992), and so it is not the most appropriate instrument with which to constrain the distribution of the WIM on CMB angular scales (~ 1 degree). Nevertheless, by summing over pixel elements in the roughly $40' \times 40'$ field-of-view, we have been able to reach a sensitivity of ~ 1 R on a scale comparable to CMB measurements. Our goal was to check for free–free emission in the region of sky where Schuster et al. (1993, SP91) and Gunderson et al. (1995, SP94) detected microwave fluctuations.

2. Observations

The observations were made in November 1996 with a 36 cm telescope in La Silla (Chile). This telescope, equipped with a scanning Fabry-Perot interferometer, is devoted to a Survey of the Milky Way and Magellanic Clouds (Amram et al. 1991, Le Coarer et al. 1992). The field of view is $38' \times 38'$; the spectral resolution was 11.5 km s^{-1} with the

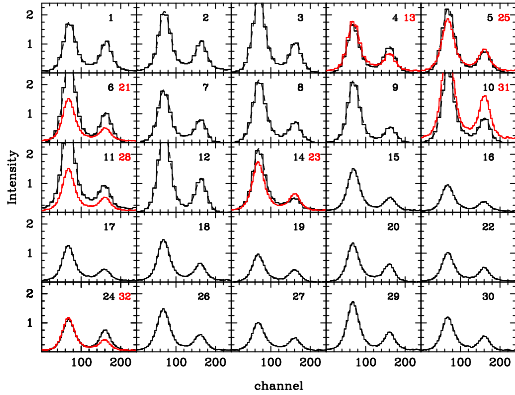


Fig. 1. Summary of the observed profiles for the different fields. The reference numbers are those of Table 2.

interferometer used here, and the sampling step was either 4.6 km s^{-1} , or 2.3 km s^{-1} (i.e. 0.10 \AA or 0.05 \AA), depending on the scanning process adopted (24 or 48 channels over the free spectral range of 115 km s^{-1} , i.e. 2.5 \AA , of the Fabry-Perot interferometer). The H α line observed was selected through a 8 \AA FWHM interference filter with 70% transmission, centered at 6563 \AA for the observing conditions. The lines passing through the filter are the Galactic H α line we are looking for, the geocoronal H α emission and the OH night sky line at 6568.78 \AA . These two parasitic lines are brighter than the Galactic H α line, the geocoronal line being typically twice as bright as the OH line and 10 times brighter than the Galactic line. The filter (3 cavities) transmission function is steep enough on the edges so that the two nearby, bright OH lines, at 6553.62 \AA and 6577.28 \AA , are effectively suppressed by the filter and may be neglected; all the more since the brighter line (6553.62 \AA) is brought into coincidence with the OH line at 6568.78 \AA , their separation being exactly 6 times the free spectral range of the Fabry-Perot.

In order to compare the Galactic H α emission fluctuations with the South Pole results (Schuster et al. 1993; Gundersen et al. 1995), we selected fields at declinations of -63° (corresponding to SP91) and -62° (corresponding to SP94). Our fields were separated by 15 mn in right ascension, which is about $1^\circ 45'$ on the sky, thus offering a fair coverage of each band. We observed 19 fields at -62° (from $\alpha = 23^{\text{h}}50^{\text{m}}$ to $\alpha =$

4^h20^m) and 6 fields at -63° (from $\alpha = 1^{\text{h}}35^{\text{m}}$ to $\alpha = 2^{\text{h}}50^{\text{m}}$). Some of these fields were observed twice, on different nights, to check the reproducibility of our measurements, and also at times with a different spectral sampling. Table 1 summarizes the observations parameters and Table 2 gives the details of these observations with exposure times and the number of scanning steps. Figure 1 shows the profiles observed in the 25 fields. The observing conditions were fairly good, with some faint cirrus clouds on the nights of November 8th, and 10th to the 13th. Only two exposures had to be cut because of heavy clouds (number 14 and 25 in Table 2), and the corresponding fields were re-observed in good conditions with the 2^h exposure time currently adopted.

3. Data reduction

Basically, we have to analyze a short spectrum, 2.52 Å wide, which is the free spectral range of our Fabry-Perot interferometer. This means in fact that the positions of the lines are known modulo 2.52 Å, and that there is some overlapping of nearby lines since we select the lines to be analyzed through an 8 Å wide interference filter. For instance, the OH night sky line at 6568.78 Å appears closer to the H α lines (geocoronal and Galactic) than it actually is, with an apparent separation of only 1 Å ($6568.78 \text{ \AA} - 6562.78 \text{ \AA} = 6.00 \text{ \AA} = 2 \times 2.52 \text{ \AA} + 0.96 \text{ \AA}$), see Figure 2 (top panel).

The Galactic H α emission is slightly separated from the geocoronal emission because of our motion with respect to the Galaxy. The motion of the Earth around the Sun and the motion of the Sun in the Galaxy were combined in such a manner that the separation between the two lines remained approximately constant, around 0.5 Å, along the bands of sky observed in November. As a result, the Galactic H α emission should appear right between the two parasitic night sky lines (geocoronal H α and OH). Its extraction is not easy, however, since it is typically 10 times fainter than the parasitic lines (see also Fig. 1 of Bartlett & Amram 1998), whose width (FWHM around 0.35 Å) and shape (not far from gaussian) also tend to bury the signal in their wings.

First of all, to improve the signal-to-noise ratio and the spectral resolution, we selected a 30' diameter disk centered on the interference rings observed in each field. This enables us to avoid the edges of the field where the interference rings are crowded and not sufficiently sampled by the pixel size of the image detector. The H α emission profile obtained for each observed field is thus the addition of the profiles of all the pixels (about 31 000) found within 15' from the center of the field.

To analyze this profile and extract the Galactic H α emission, we must know precisely the shape of each line to be subtracted. The OH night sky line at 6568.78 Å is in fact the sum of two close components of the same intensity, one at 6568.77 Å and the other at 6568.78 Å. This fine structure can be neglected here, and the line may be considered as a single line. More complicated is the case of the geocoronal emission line, with not less than seven fine structure transitions. The two main components, produced by Lyman β resonance excitation, are found at 6562.73 Å and 6562.78 Å, with a 2:1 ratio (Yelle & Roesler 1985). The resulting line center, at 6562.74 Å, is different from that in a discharge lamp (6562.79 Å), where all fine structure levels are excited. However, these two components proved insufficient when we decomposed our observed profiles, a residual remaining systematically at 6562.92 Å. This is due to cascade excitation which is particularly strong for the 7th component at 6562.92 Å (Nossal 1994). Although the percentage of cascade contribution is not accurately known, it proved satisfactory to use the Meier model cited in Nossal's thesis, adding a component at 6562.92 Å with a 1:6 ratio compared with the brightest component at 6562.73 Å. To summarize, then, we decomposed the H α geocoronal emission into three components : 6562.73 Å, 6562.78 Å (with intensity ratio 1:2) and 6562.92 Å (with intensity ratio 1:6).

The night sky line profiles are narrow and fairly well reproduced by the instrumental profile. This profile is obtained by scanning the emission line of a Neon lamp at 6598.95 Å during two hours.

We can thus subtract the OH line and geocoronal H α components from our observed profile since we know their positions, the only free parameter being the intensity (remember, however, that the *relative* intensities of the three main components we considered for the geocoronal H α line are kept fixed at 1, 1:2, 1:6). After subtraction of the night sky lines, a residual was found at the expected velocity for Galactic H α emission, that is to say around zero in V_{LSR} (radial velocity in the local standard of rest) and with the expected width, around 35 km s⁻¹, in good agreement with Reynolds' (1990) results. Figure 2 shows an example of profile decomposition for one of our fields, together with a gaussian fit to the Galactic emission below. The width of the gaussian was left as a free parameter and adjusted automatically for the best fit. This width was typically found to lie between 25 and 50 km s⁻¹ (see Table 2). For 7 out of our 32 observations, the signal-to-noise ratio was too faint for a good fit, and we imposed the average width (~ 35 km s⁻¹).

We scanned many fields with 48 steps, instead of the usual 24 steps, in order to check the interest of oversampling. Because of the *Finesse* of our Fabry-Perot interferometer (about 10 at H α), the usual sampling criteria indicate that 24 scanning steps are sufficient to obtain profiles with the best achievable resolution. However, oversampling is sometimes

necessary, especially when decomposing a profile into several close components. Indeed, we found no significant difference between the observations at 48 scanning steps and those at 24 steps, although the profiles drawn with 48 steps are smoother, precisely because of the better sampling.

The calibration in intensity was made by observing through the same instrument (although through a slightly redshifted H α interference filter) the HII region N11E in the Large Magellanic Cloud, for which an absolute calibration has been performed by Caplan & Deharveng (1985).

Let us note that we also used a rough method which produced nearly the same intensity variations. This method consists of assuming that the night sky lines are symmetric; then, taking into account the left wing of the geocoronal H α line, which is contaminated by neither the Galactic emission nor the OH, one can infer that the right wing is its mirror image. Similarly, one considers the right wing of the OH night sky line, which is not contaminated by either Galactic emission or geocoronal H α , and assumes that the left wing is its mirror image. The Galactic H α emission is then deduced from the subtraction of these two symmetric lines. The results are not significantly different from the results obtained with our more sophisticated method.

4. Results

We find an intensity of Galactic emission in the observed bands, at -62° and -63° , varying between 0.2 R and 1.4 R (see Table 2), in good agreement with intensity values measured by Reynolds (1990) in the northern hemisphere far from the Galactic plane.

Figure 3 shows the measured intensity of Galactic H α at declination $\delta = -62^\circ$ and $\delta = -63^\circ$. The error bars are the average rms difference between the signal and the fitted gaussian, found to be 0.35 Rayleigh. We note that Reynolds (1990) quotes comparable uncertainties, ~ 0.4 Rayleigh.

To check the reproducibility of our observations, we observed seven fields twice. The differences in intensity we found for these fields vary by 40% in average, with just 0.4 Rayleigh as an average value, close to the uncertainty mentioned above. For the seven fields observed twice, the corresponding differences in intensity are (in % and in increasing order): 15, 21, 28, 43, 47, 52 and 79. The 43% difference may be easily explained by meteorologic effects, the lower intensity value having been obtained in bad conditions (the exposure had to be cut at 2640s because of clouds). The strong 79% difference may be explained, at least partially, by a 10' drift of the field due to the loss of the guide star at mid-exposure. However, the remaining 47 and 52% differences are abnormally large and cannot be explained by observing conditions.

Figure 3 suggests that the overall variations are small and that the galactic H α emission varies smoothly along the two bands of sky observed.

5. Discussion and conclusions

The goal of these observations was to constrain and quantify the possible Galactic free-free contamination of the SP91 and SP94 CMB results. The former consists of data taken along a strip at -63° declination over a narrow range of frequencies centered on 30 GHz (K band), and which show a falling signal more characteristic of free-free emission than of the CMB. The SP94 scan being adjacent in declination, we also chose to observe along this band at $\delta = -62^\circ$, although these data were taken in both K and Q (38 – 40 GHz) bands and show fluctuations consistent with a thermal spectrum (CMB).

The absolute intensity of the total H α emission over the observed bands is quite low (mean = 0.85 R and maximum < 1.5 R), with variations equal to our estimated uncertainty of ~ 0.35 R. As mentioned, this is consistent with previous work using both interferometers and narrow band filters. If we assume the WIM producing our signal is indeed at $T \sim 10^4$, then Eq. (4) indicates that it contributes at most $\sim 10\mu\text{K}$ to the SP results in the K band. For comparison, the two largest fluctuations in SP91, those dominating the signal attain $\sim 50\mu\text{K}$, while the *rms* level seen in SP94 is $\sim 40\mu\text{K}$. A comparison of our H α results and the SP data sets is given in Figure 4, again using Eq. (4). It must be remembered that the SP points in this figure are really differences between fields adjacent on the sky, while the H α points represent absolute intensities at the given positions. Our results imply that, at a temperature of a few 10^4 K, the corresponding free-free emission is smaller than about $10\mu\text{K}$ at 30 GHz (K band), and hence does not significantly contaminate the SP experiments. It is worth mentioning, however, two possibilities which could lead to more important contamination of CMB signals despite low measured H α intensities. Firstly, the above discussion assumes that the WIM does not have a higher temperature component. We note that even ~ 0.5 R variations, allowed at the $\sim 2\sigma$ -level, from a gas at $\sim 10^6$ K would produce fluctuations in K-band comparable to those observed in the SP data sets; the spectral information from the SP94 observations makes this seem unlikely, however. Secondly, it may well be that an important source of foreground to the contamination arises not from Bremsstrahlung, but from the rotational emission of very small spinning dust grains (Draine & Lazarian 1998). In this case, a correlation between the 30 GHz emission and the diffuse $12\mu\text{m}$ emission is expected. It remains to be seen whether these two effects will indeed be significant.

Acknowledgements

We thank the participants to the meeting organised in November 1995 by D. Valls-Gabaud and J.P. Sivan at the Observatoire de Haute Provence, for stimulating discussions.

References

- Amram, P., Boulesteix, J., Georgelin, Y.M. et al., 1991, *Messenger*, 64, 44.
- Bartlett, J.G. & Amram, P. 1998, in “Fundamental Parameters in Cosmology”, Moriond proceedings, in press, *astro-ph/9804330*
- Caplan, J. & Deharveng, L. 1985, *A&AS* 62, 63
- Draine, B.T. & Lazarian, A. 1998, *ApJ* 494, L19
- Gaustad, J.E., McCullough, P.R. & Van Buren, D. 1996, *PASP* 108, 351
- Gundersen, J.O., Lim, M., Staren, J., et al. 1995, *ApJ* 443, L57
- Haslam, C.G.T., et al. 1981, *A&A* 100, 209
- Jungman, G., Kamionkowski, M., Kosowsky, A. & Spergel, D.N. 1996, *Phys. Rev. Lett.* 76, 1007
- Le Coarer, E., Amram, P., Boulesteix, J. et al. 1992, *A&A* 257, 389
- Knox, L. 1995, *Phys. Rev. D* 52, 4307
- Kogut, A., Banday, A.J., Bennett, C.L., Górski, K.M., Hinshaw, G. & Reach, W.T. 1996a, *ApJ* 460, 1
- Kogut, A., Banday A.J., Bennett, C.L., Górski, K.M., Hinshaw, G., Smoot, G.F. & Wright, E.L. 1996b, *ApJ* 464, L5
- Leitch, E.M., Readhead, A.C.S., Pearson, T.J. & Myers, S.T. 1997, *ApJ* 486, L23
- Lineweaver, C.H., Barbosa, D., Blanchard, A. & Bartlett, J.G. 1997, *A&A* 322, 365
- Netterfield, C.B. et al. 1997, *ApJ* 474, 47
- Nossal, S. 1994, PhD. thesis, University of Wisconsin, Madison
- Reich, P. & Reich, W. 1986, *A&AS* 63, 205
- Reynolds, R.J. 1980, *ApJ* 236, 153
- Reynolds, R.J. 1990, IAU symposium “The Galactic and Extragalactic Background Radiation”, Eds. S. Bower & C. Leinert, 157
- Reynolds, R.J. 1992, *ApJ* 292, L35
- Schuster, J., Gaier T., Gundersen, J., Meinhold P., Koch, T., Seiffert, M., Wuensche, C.A. & Lubin, P. 1993, *ApJ* 412, L47
- Simonetti, J.H., Dennison, B. & Topasna, G.A. 1996, *ApJ* 458, L1
- Smoot, G.F. et al. 1992, *ApJ* 396, L1
- Smoot, G. 1998, *astro-ph/9801121*
- Valls-Gabaud, D. 1998, *PASA* 15, 111
- White, M., Scott, D. & Silk, J. 1994, *ARA&A* 32, 319
- Wollack, E.J. et al. 1997, *ApJ* 476, 440
- Yelle, R.V. & Roesler, F.L. 1985, *J. Geophys. Res.* 90, 7568

Table 1. Observations parameters

Observations	Telescope	Marseille 36 cm
	Location	La Silla
	Equipment	CIGALE Cassegrain focus
	Date	Nov 1996
Interference Filter	Central wavelength at 10°C	6566 Å
	Transmission	0.68
	FWHM	8 Å
Calibration	H α Comparison light	λ 6562.78 Å
Perot–Fabry	Interference order	2604 @ 6562.78 Å
	Free spectral range	115 km s ⁻¹
	Finesse at H α	10
Spectral Sampling	24 Scanning steps	0.105 Å (4.6 km s ⁻¹)
	48 Scanning steps	0.052 Å (2.3 km s ⁻¹)
Spatial Sampling	Total field	38' \times 38' (256 \times 256 px ²)
	Useful circular field	ϕ 30'
	Pixel size	9.1''
Typical exposures times	Total exposure	2 hours
	Elementary scanning exposure time	5 s per channel
	Total exposure time per channel	300 s

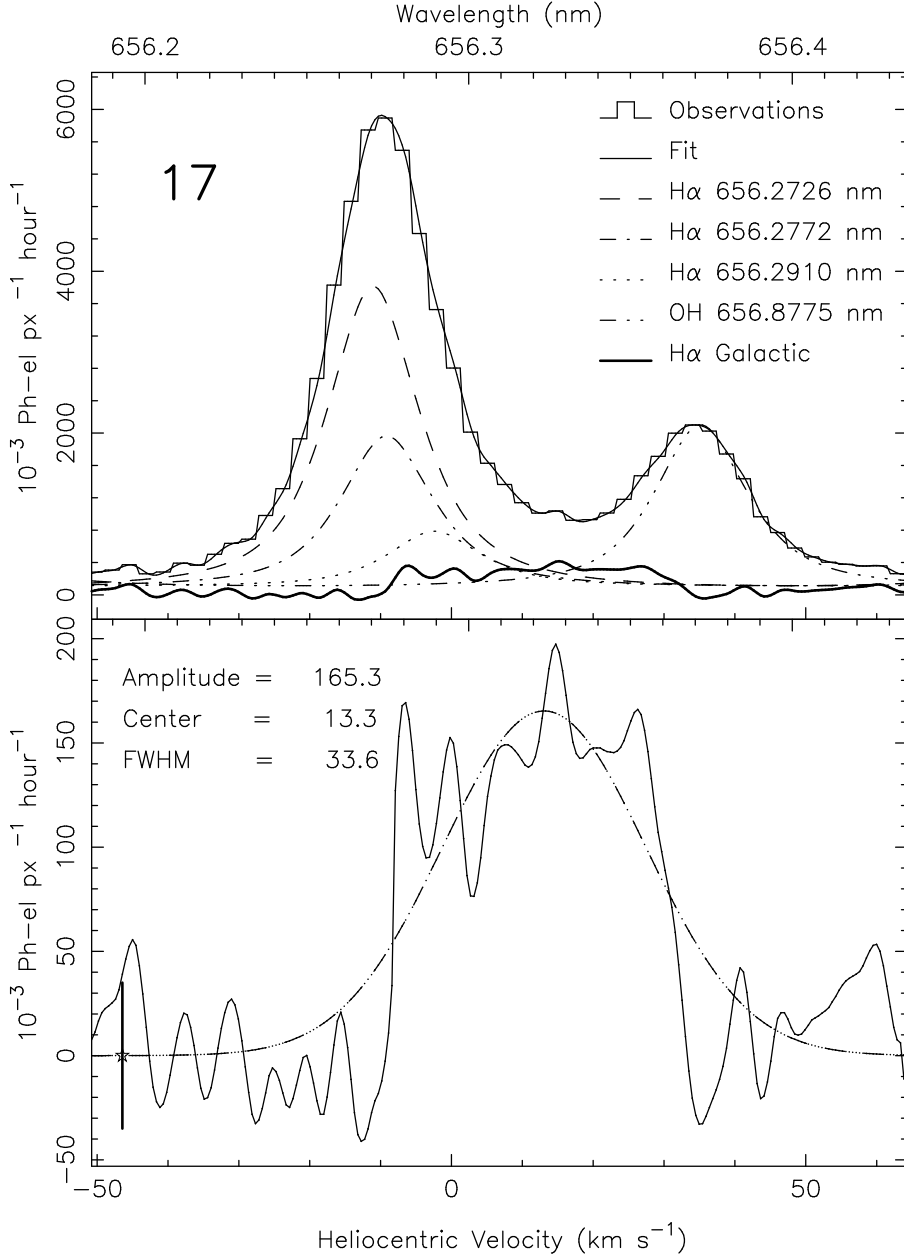


Fig. 2. Top: Example of decomposition of the observed line profile, for reference field 17 (see Table 2), into geocoronal H α emission (3 components) and OH night sky line. The remaining signal (thick line) shows the Galactic H α emission. Bottom: Best fit of the Galactic H α emission by a gaussian profile. The shift with respect to the 0 km s $^{-1}$ heliocentric velocity is due to the motion with respect to the LSR.

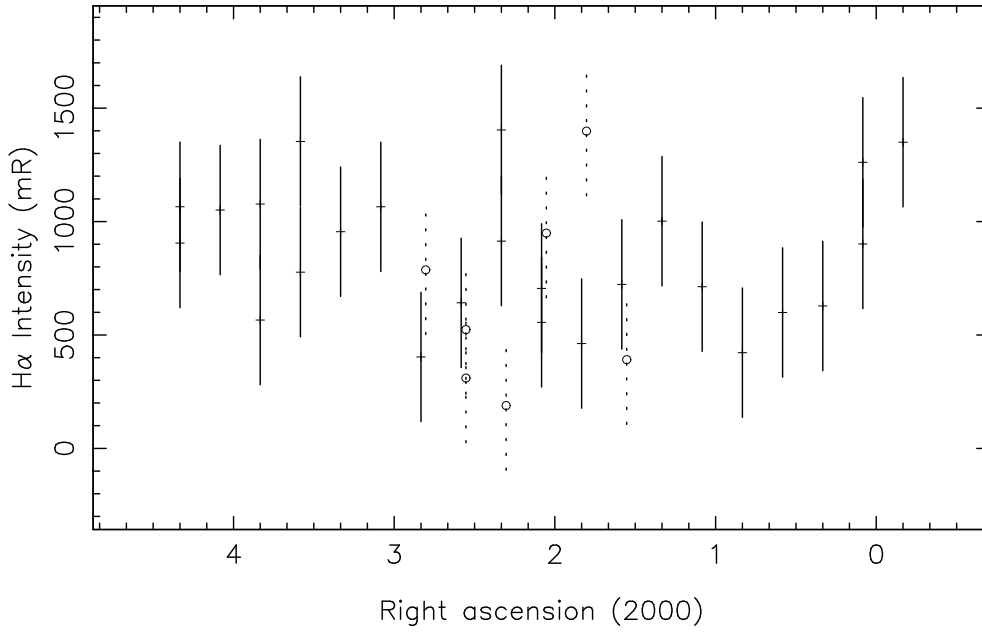


Fig. 3. H α intensities measured at declination -62° (full lines) and at declination -63° (dotted lines).

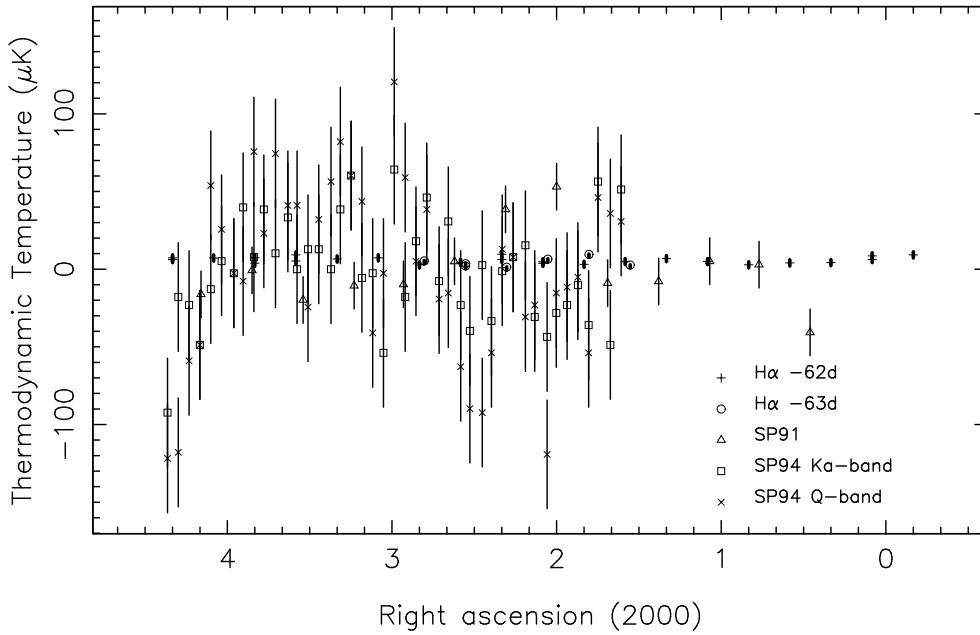


Fig. 4. Comparison of the SP results with the free-free emission signal deduced from our H α observations

Table 2. Observed Fields

Reference number	Coordinates (2000)		Date	t_{exp} s	N_{scans}	I(H α) mR	FWHM km s $^{-1}$	V_{LSR} km s $^{-1}$
	α	δ						
3	23 ^h 50 ^m	-62°	Nov 5 1996	7200	24	1350	40	-1
6	0 ^h 05 ^m	-62°	Nov 6 1996	7200	24	1261	48	-5
21		-62°	Nov 11 1996	7200	48	901	31	+1
9	0 ^h 20 ^m	-62°	Nov 7 1996	7200	24	628	72	-2
12	0 ^h 35 ^m	-62°	Nov 8 1996	7200	24	599	34	-8
15	0 ^h 50 ^m	-62°	Nov 9 1996	7200	48	422	27	+4
18	1 ^h 05 ^m	-62°	Nov 10 1996	7200	48	713	34	-2
7	1 ^h 20 ^m	-62°	Nov 6 1996	7200	24	1002	35	+4
1	1 ^h 35 ^m	-62°	Nov 4 1996	7200	24	723	34	+10
2	1 ^h 50 ^m	-62°	Nov 4 1996	7200	24	462	38	+7
4	2 ^h 05 ^m	-62°	Nov 5 1996	7200	24	705	35	+12
13		-62°	Nov 8 1996	7200	24	556	34	+10
10	2 ^h 20 ^m	-62°	Nov 7 1996	7200	24	914	36	+8
31		-62°	Nov 15 1996	7680	48	1404	46	+8
16	2 ^h 35 ^m	-62°	Nov 9 1996	7200	48	642	30	+7
19	2 ^h 50 ^m	-62°	Nov 10 1996	7200	48	403	26	+13
20	3 ^h 05 ^m	-62°	Nov 10 1996	7200	48	1065	34	+13
17	3 ^h 20 ^m	-62°	Nov 9 1996	7200	48	955	30	+13
14	3 ^h 35 ^m	-62°	Nov 8 1996	2640	24	777	31	+14
23		-62°	Nov 11 1996	7200	48	1353	35	+11
11	3 ^h 50 ^m	-62°	Nov 7 1996	7200	24	1077	35	+13
28		-62°	Nov 13 1996	7200	48	566	34	+15
8	4 ^h 05 ^m	-62°	Nov 6 1996	7200	24	1051	29	+10
5	4 ^h 20 ^m	-62°	Nov 5 1996	7200	24	1065	46	+14
25		-62°	Nov 12 1996	6960	48	905	28	+11
22	1 ^h 35 ^m	-63°	Nov 11 1996	7200	48	391	28	+6
26	1 ^h 50 ^m	-63°	Nov 13 1996	7200	48	1399	38	0
27	2 ^h 05 ^m	-63°	Nov 13 1996	7200	48	949	29	+7
29	2 ^h 20 ^m	-63°	Nov 14 1996	7200	48	189	34	-6
24	2 ^h 35 ^m	-63°	Nov 12 1996	7200	48	310	26	+1
32		-63°	Nov 15 1996	7200	48	524	34	+12
30	2 ^h 50 ^m	-63°	Nov 14 1996	7200	48	787	28	+3